ARTICLE
Journal of Cellular Biochemistry 112:840–848 (2011)

Journal of Cellular Biochemistry

Bioluminescence Reporter Gene Imaging Characterize Human Embryonic Stem Cell-Derived Teratoma Formation

Weijun Su,[1] Manqian Zhou,[1] Yizhou Zheng,[3] Yan Fan,[1] Lina Wang,[1] Zhongchao Han,[3] Deling Kong,[5] Robert Chunhua Zhao,[5] Joseph C. Wu,[6] Rong Xiang,[1*] and Zongjin Li[2,4*]

[1]*Department of Immunology, Nankai University School of Medicine, Tianjin, China*

[2]*Department of Pathophysiology, Nankai University School of Medicine, Tianjin, China*

[3]*State Key Lab of Experimental Hematology, Institute of Hematology and Hospital of Blood Diseases, Chinese Academy of Medical Sciences, Tianjin, China*

[4]*The Key Laboratory of Bioactive Materials, The College of Life Science, Nankai University, Ministry of Education, Tianjin, China*

[5]*Institute of Basic Medical Sciences and School of Basic Medicine, Center of Excellence in Tissue Engineering, Chinese Academy of Medical Sciences and Peking Union Medical College, Beijing, China*

[6]*Division of Cardiology, Department of Medicine, Stanford University School of Medicine, Stanford, CA 94305*

ABSTRACT

Human embryonic stem (hES) cells have a potential use for the repair and regeneration of injured tissues. However, teratoma formation can be a major obstacle for hES-mediated cell therapy. Therefore, tracking the fate and function of transplanted hES cells with noninvasive imaging could be valuable for a better understanding of the biology and physiology of teratoma formation. In this study, hES cells were stably transduced with a double fusion reporter gene consisting of firefly luciferase and enhanced green fluorescent protein. Following bioluminescence imaging and histology, we demonstrated that engraftment of hES cells was followed by dramatically increasing signaling and led to teratoma formation confirmed by histology. Studies of the angiogenic processes within teratomas revealed that their vasculatures were derived from both differentiated hES cells and host. Moreover, FACS analysis showed that teratoma cells derived from hES cells expressed high levels of CD56 and SSEA-4, and the subcultured SSEA-4$^+$ cells showed a similar cell surface marker expression pattern when compared to undifferentiated hES cells. We report here for the first time that SSEA-4$^+$ cells derived from teratoma exhibited multipotency, retained their differentiation ability in vivo as confirmed by their differentiation into representative three germ layers. J. Cell. Biochem. 112: 840–848, 2011.

KEY WORDS: BIOLUMINESCENCE IMAGING; REPORTER GENE; HUMAN EMBRYONIC STEM CELLS; DIFFERENTIATION; TERATOMA FORMATION

Since it was first reported that human embryonic stem (hES) cells propagate as individual lines in vitro in 1998 [Thomson et al., 1998], such cells attracted enormous attention for their potential use as raw material for the production of therapeutically useful cell types. However, most preparations of differentiated hES cells are merely enriched for the cell type of interest, and the presence of unknown, confounding, and possible tumor-promoting cell types raised concerns about the safety of their clinical applications [Hentze et al., 2009]. The ability of hES cells to form noncancerous tumors called teratomas is one of their defining traits. Moreover, several studies have shown that hES cells which differentiated for extended periods of time are still able to form

Weijun Su and Manqian Zhou contributed equally to this work.

Grant sponsor: National Key Scientific Program of China; Grant numbers: 2011CB964903, 2007CB914804; Grant sponsor: National Natural Science Foundation of China; Grant number: 31071308; Grant sponsor: National Development Plan of High Technology of China; Grant number: 2007AA021010; Grant sponsor: The National Institutes of Health; Grant number: HL091453, AI085575; Grant sponsor: National Natural Science Foundation of China; Grant number: 30830096; Grant sponsor: Tianjin Municipal Science and Technology Commission; Grant number: 09ZCZDSF04000.

*Correspondence to: Rong Xiang, MD, PhD, and Zongjin Li, MD, PhD, Nankai University School of Medicine, 94 Weijin Road, Tianjin, China, 300071. E-mail: rxiang@nankai.edu.cn; lizongjin@hotmail.com

Received 19 October 2010; Accepted 24 November 2010 • DOI 10.1002/jcb.22982 • © 2010 Wiley-Liss, Inc.
Published online 7 December 2010 in Wiley Online Library (wileyonlinelibrary.com).

teratoma [Phillips et al., 2007; Xu et al., 2008; Hentze et al., 2009]. This also is of concern, particularly for those investigators who hope to develop therapies from these cells.

To fully comprehend the mechanism of hES cell therapy, one would have to understand the dynamic process of cell homing, migration, biodistribution, proliferation, and differentiation overtime in the same subject. Therefore, the development of noninvasive and sensitive in vivo tracking technologies may will play an indispensable role in detailed preclinical studies to optimize delivery methods and strategies which can monitor the behavior of hES cells after transplantation [Li et al., 2009a]. Reporter gene imaging, is useful in assessing kinetic survival status of the implanted cells because reporter gene(s) can be expressed as long as the cells are alive, and inserted reporter gene(s) can be passed on to daughter cells upon cell division [Li et al., 2007, 2008]. Among the different reporter gene(s) imaging techniques, bioluminescence imaging (BLI) is of considerable use because of its sensitivity, high-throughput screening, and straightforward imaging procedures [Li et al., 2009a].

Tumor angiogenesis is the proliferation of a network of blood vessels that penetrate into cancerous growths, supplying nutrients and oxygen, and removing waste products. The discovery and characterization of teratoma-derived angiogenesis processes will greatly contribute to our understanding of how teratoma regulates angiogenesis and will provide therapeutic strategies for teratoma formation after hES cell therapy.

Here, hES cells were stably transduced with a lentiviral vector carrying novel double-fusion (DF) reporter genes consisting of firefly luciferase (Fluc), enhanced green fluorescence protein (GFP), while hES cells were simultaneously transplanted into mice hindlimbs. BLI was used to track the Fluc-labeled hES cells. Moreover, both the angiogenesis of teratoma and characterization of teratoma-derived cells were accomplished.

MATERIALS AND METHODS

MAINTENANCE OF HUMAN EMBRYONIC STEM CELLS

Undifferentiated hES cells (H9 line from Wicell, Madison, WI; Passages 38–45) were grown on an inactivated mouse embryonic fibroblast feeder layer as previously described [Li et al., 2008, 2009c].

LENTIVIRAL TRANSDUCTION OF hES CELLS WITH DF REPORTER GENE

In order to track transplanted cells in vivo, hES cells were transduced at multiplicity of infection of 10 with self-inactivating (SIN) lentiviral vector carrying a human ubiquitin promoter driving Fluc and enhanced GFP (Fluc-GFP) [Li et al., 2008, 2009c]. Stable clones were isolated using FACS for GFP expression. Afterwards, Fluc activity within different cell numbers was confirmed ex vivo with a Xenogen IVIS 200 system (Xenogen, Alameda, CA) as described [Li et al., 2008, 2009c]. To test expression patterns of stem cell marker Oct-4, nontransduced hES cells (control) and hES cells with DF reporter genes (hESC-DF) were stained for Oct-4 (Chemicon, Temecula, CA).

TRANSPLANTATION OF hES CELLS INTO MURINE HINDLIMBS

All procedures were performed on 9–12 week old female SCID mice (Laboratory Animal Center of the Academy of Military Medical Science, Beijing, China) ($n = 10$) according to guidelines of the Nankai University Animal Care and Use Committee. Mice were anesthetized by intraperitoneal injection of ketamine (100 mg/kg) and xylazine (20 mg/kg). Approximately 1×10^6 undifferentiated hES cells (stably transduced with DF reporter genes) were injected into left hind limbs in 50 μl PBS. 1×10^6 human umbilical cord mesenchymal stem cells (MSC) [Zhao et al., 2009] stably transduced with DF reporter genes were used as control and injected into right hind limbs.

FLOW CYTOMETRY SORTING OF TERATOMA-DERIVED CELLS

Mice were euthanized after cell transplantation at day 28 and single teratoma cells were isolated. Briefly, mice were saturated with alcohol, and teratomas were separated from skeletal muscle with sterilized instruments. Then the teratomas were placed in a new culture plate, washed with PBS, and minced with curved dissecting scissors into grain sized pieces. Single cell suspensions of teratoma were obtained by subsequent treatment with 0.56 units/ml of Liberase Blendzyme IV (Roche, Indianapolis) at 37 °C for 20–30 min. Cells were passed through a 40-μm cell strainer [Xu et al., 2006]. Antibodies used in this study were phycoerythrin conjugated anti-CD31 (BD Pharmingen), allophycocyanin (APC) conjugated anti-CD56 (BD), APC conjugated anti-KDR (R&D Systems), APC conjugated with anti-CD133 (R&D Systems), APC conjugated anti-mouse IgG/IgM, anti-rat IgM, and rat anti-human SSEA-3 (Chemicon) as well as mouse anti-human SSEA-4, TRA-1-60, and TRA-1-81 (Chemicon). The stained cells were analyzed using FACS Vantage (Becton-Dickinson, MA). $GFP^+/SSEA\text{-}4^+$ cells were isolated and subcultured on Matrigel-coated plates in mTeSR1 medium (Stem Cell Technologies, Vancouver, BC, Canada). $GFP^+/SSEA\text{-}4^+$ cells were subcultured by treating with collagenase type IV and scraped mechanically.

TRANSPLANTATION OF TERATOMA-DERIVED CELLS INTO MURINE HINDLIMBS

The proliferation activity and multipotency of hES cells derived from teratoma has not been determined in vivo before. To further investigate in vivo behavior of teratoma-derived cells, approximately 1×10^6 $GFP^+/SSEA\text{-}4^+$ cells were injected into left hind limbs of SCID mice ($n = 10$) in 50 μl PBS as mentioned above.

OPTICAL BIOLUMINESCENCE IMAGING OF TRANSPLANTED CELL FATE IN LIVING MICE

BLI was performed using the Xenogen IVIS 200 system. After intraperitoneal injections of reporter probe D-luciferin (150 mg luciferin/kg), animals were imaged for periods of 2 s to 2 min. The same mice were scanned for 4 weeks after transplantation of hES cells and 10 weeks after transplantation of $GFP^+/SSEA\text{-}4^+$ teratoma-derived cells. Imaging signals were quantified in units of maximum photons/s/cm^2/steridian (photons/s/cm^2/sr) as previously described [Li et al., 2009b].

IMMUNOHISTOCHEMICAL STAINING FOR ANGIOGENESIS OF TERATOMA

At week 4, separated teratomas were embedded into OCT compound (Miles Scientific) and frozen sections (5 μm thick) were processed for immunostaining. Angiogenesis of teratoma was investigated with rabbit anti-GFP antibody (Invitrogen), mouse anti-human CD31 antibody (BD Pharmingen), and rat anti-mouse CD31 antibody (BD Pharmingen). Alexa Fluor 488, and Alexa Fluor 594-conjugated secondary antibodies were applied appropriately. DAPI was used for nuclear counterstaining. H&E staining was also performed to identify the fate of transplanted hES cells. The behavior of transplanted GFP^+/$SSEA\text{-}4^+$ teratoma-derived cell was explored by staining the neoplasm separated from hind limbs with H&E at day 70.

STATISTICAL ANALYSIS

ANOVA and two-tailed Student's *t*-test were used and differences were considered significant at *P*-values of <0.05.

RESULTS

GENERATION OF hES CELLS WITH DF REPORTER GENES

We developed an imaging platform for tracking hES cells in mice by using DF reporter genes consisting of Fluc-GFP. DF reporter genes were cloned into a SIN lentiviral vector downstream from the constitutive ubiquitin promoter (Fig. 1A). Both control nontransduced hES cells and stably transduced hES cells showed similar expression patterns of stem cell marker Oct-4 on immunostaining, suggesting negligible side effects by reporter genes during maintenance of the stem cell state (Fig. 1B). After culture in 24-well plates, we also observed a strong correlation ($\gamma^2 = 0.99$) between Fluc activity and cell numbers ex vivo when using the Xenogen IVIS system (Fig. 1C). Moreover, there was no difference between nontransduced cells and transduced hES cells respective to cell proliferation and cell viability (data not shown). In general, these data are consistent with those of prior study in which hES cells with double fusion reporter genes did not differ from nontransduced hES cells on cell with regarding cell survival, proliferation, and differentiation [Li et al., 2008].

LONGITUDINAL REPORTER GENE IMAGING OF hES CELL SURVIVAL IN LIVING ANIMALS

We assessed stem cell fate with reporter genes imaging by injecting approximately 1×10^6 hES cells stably transduced with DF reporter genes into left hind limbs of mice in 50 μl PBS. Human umbilical cord MSC 1×10^6 stably transduced with DF reporter genes were injected into right hind limbs as a control. After injection, longitudinal BLI was performed on these animals for 4 weeks (Fig. 2A). In both hind limbs, bioluminescence signals were robust on day 2 after injection. In the MSC group, bioluminescence signals progressively decreased from day 2 to day 28, indicating acute MSC death. Different from the survival pattern of the MSC group, the bioluminescence signals of the hES cell group first showed a sharp drop from day 2 to day 7, which was followed by a dramatic increase in the following 3 weeks. At the end of the week 4, signals of hES cells were approximately 20-fold higher than those observed on day 2 (Fig. 2B). This specific pattern of hES cells death, followed by cell proliferation was seen in most animals analyzed.

POSTMORTEM HISTOLOGY AND IMMUNOHISTOCHEMISTRY OF TERATOMA

All animals were sacrificed 4 weeks after hES cells transplantation. Histologic analysis showed teratoma formation of hES cells (Fig. 2C-I) and H&E staining of teratoma formation after hES cell implantation identified various differentiated cells representative of the three embryonic germ layers, such as neural epithelium representatives of the ectoderm (Fig. 2C-II), osteoid formation representative of the mesoderm (Fig. 2C-III), and gut epithelium for endoderm (Fig. 2C-IV), as well as immature components.

To investigate angiogenesis of teratoma, we first immunostained for GFP and human CD31 on teratoma derived from transplanted double fusion hES cells. We found that vascular-like structures co-expressed GFP and human CD31, indicating endothelial differentiation of the transplanted GFP positive hES cells in vivo (Fig. 3A). Next, we immunostained for GFP and mouse CD31. We observed that vascular networks inside the teratoma expressed mouse CD31 but not GFP, indicating their host-derived origin (Fig. 3B).

SUBCULTURE AND CHARACTERIZATION OF TERATOMA-DERIVED CELLS

On day 28 after cell transplantation, we euthanized the mice and obtained single cell suspensions of teratomas. Flow cytometric analysis showed that more than 90% of the teratoma cells expressed GFP, indicating that those cells were derived from hES cells (Fig. 4A). Flow cytometric analysis revealed that teratoma expressed a panel of differentiated (CD31, CD133, KDR, and CD56) as well as undifferentiated markers (SSEA-3, SSEA-4, Tra-1-60, and Tra-1-81). Especially, CD56 ($85 \pm 10.2\%$) and undifferentiated marker SSEA-4 ($12.1 \pm 2.7\%$) were expressed at high level (Fig. 4B). We then isolated the GFP^+/$SSEA\text{-}4^+$ cells and subcultured this cell population on Matrigel-coated plates in mTeSR1 medium. The morphology of GFP^+/$SSEA\text{-}4^+$ teratoma-derived cells was like that of undifferentiated hES cells and was GFP positive (Fig. 4C). Immunostaining data revealed that the teratoma-derived GFP^+/$SSEA\text{-}4^+$ cells expressed a low level of Oct-4 compared to undifferentiated hES cells (data not shown). Flow cytometric analysis showed that the GFP^+/$SSEA\text{-}4^+$ cells had similar cell surface marker expression pattern compared to undifferentiated hES cells. However, the GFP^+/$SSEA\text{-}4^+$ cells expressed a very high level of CD56, but a lower level of undifferentiated markers, such as SSEA-3, SSEA-4, TRA-1-60, and TRA-1-81 (Fig. 4D).

We next injected approximately 1×10^6 GFP^+/$SSEA\text{-}4^+$ teratoma-derived cells into the left hind limbs of SCID mice and performed longitudinal BLI on these animals for 10 weeks. Similar to mice injected with hES cells, the same characteristic special pattern of cell death, followed by cell proliferation, was also observed in mice injected with GFP^+/$SSEA\text{-}4^+$ cells. However, the latter population proliferated at a relatively lower rate. A representative animal injected with GFP^+/$SSEA\text{-}4^+$ cells showed significant bioluminescence activity at day 2, which decreased during the first 7 days and then increased progressively over the following 10 weeks. At the end of the tenth week, the signals of teratoma cells were approximately 15-fold higher than those observed on day 2 (Fig. 5A,B).

Upon injection into SCID mice, GFP^+/$SSEA\text{-}4^+$ cells formed teratoma again in vivo. But, the GFP/$SSEA\text{-}4^+$ cells derived

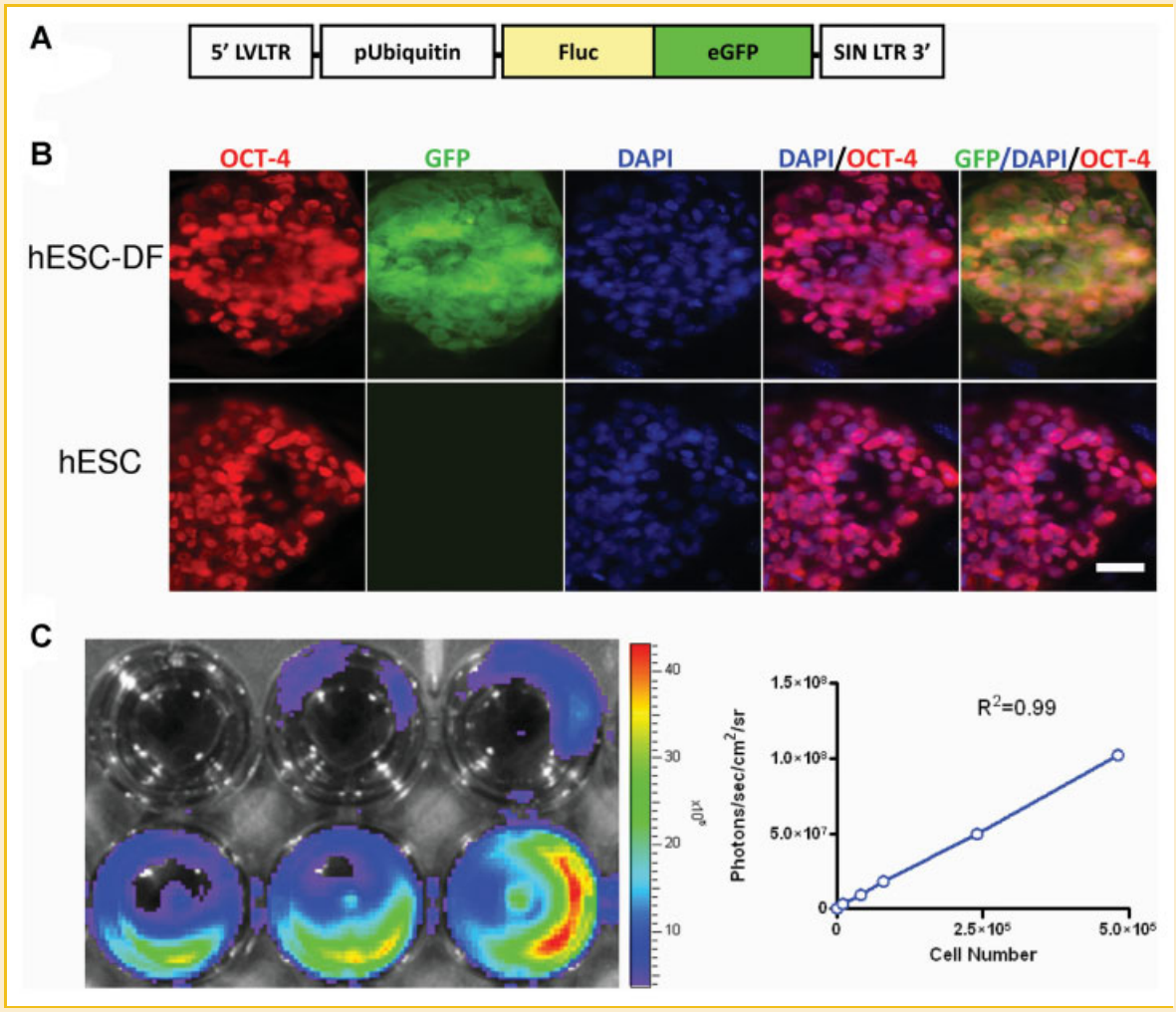

Fig. 1. Stable lentiviral transduction of hES cells with the double fusion reporter genes. A: Schema of the double fusion reporter gene containing fusion of Fluc-GFP. The double fusion reporter gene was cloned into a SIN lentiviral vector downstream from the constitutive ubiquitin promoter. B: Control nontransduced hES cells and transduced hES cells (hESC-DF) showed similar expression pattern of Oct-4 under fluorescence microscopy. DAPI staining is used as a nuclear marker. Scale bar = 20 μm. C: Ex vivo imaging analysis of stably transduced hES cells show increasing bioluminescence signals with cell numbers of hES cells ($r^2 = 0.99$).

teratomas were smaller (2.1 ± 1.0 mm) compared to hES cells derived teratomas (10.0 ± 1.5 mm) ($P < 0.01$). The postmortem histological analysis showed that the neoplasm from GFP^+/$SSEA\text{-}4^+$ cells also contained tissues of all three embryonic germ layers, such as neural epithelium representative of ectoderm (Fig. 5C-I), adipose tissue representative of mesoderm (Fig. 5C-III), and gut epithelium representative of endoderm (Fig. 5C-IV). However, when comparing hES cells derived teratoma, the latter one contained more mature components with a lower nuclear-to-cytoplasmic ratio.

DISCUSSION

To make the next quantum leap in stem cell research, it is imperative to understand the dynamic processes of hES cell homing, migration, biodistribution, proliferation, and differentiation in the same subject over time. Here, we could determine the kinetics of cell survival over time within the same individual. Thus we transduced hES cells with a double fusion reporter genes consisting of Fluc-GFP to track such cells in vivo. We observed no apparent side effects by the reporter genes on maintaining stem cell state, cell viability, and cell proliferation. Additionally, a close relationship was observed between hES cell numbers and luciferase activity, which indicates that noninvasive imaging of Fluc-GFP-labeled hES cells provides a sensitive and simple means to observe the presence of engrafted hES cells. In this way it becomes practicable to monitor the kinetics of hES cells before palpable teratomas are formed which typically takes several weeks.

hES cells are remarkable for their unlimited self-renewal and pluripotency capacity and an obstacle to their therapeutic use is teratoma formation. Tumor growth, including teratoma, requires a network of blood vessels to maintain nutritional supplement and antiangiogenic therapy to limit or even reverse the growth of tumors

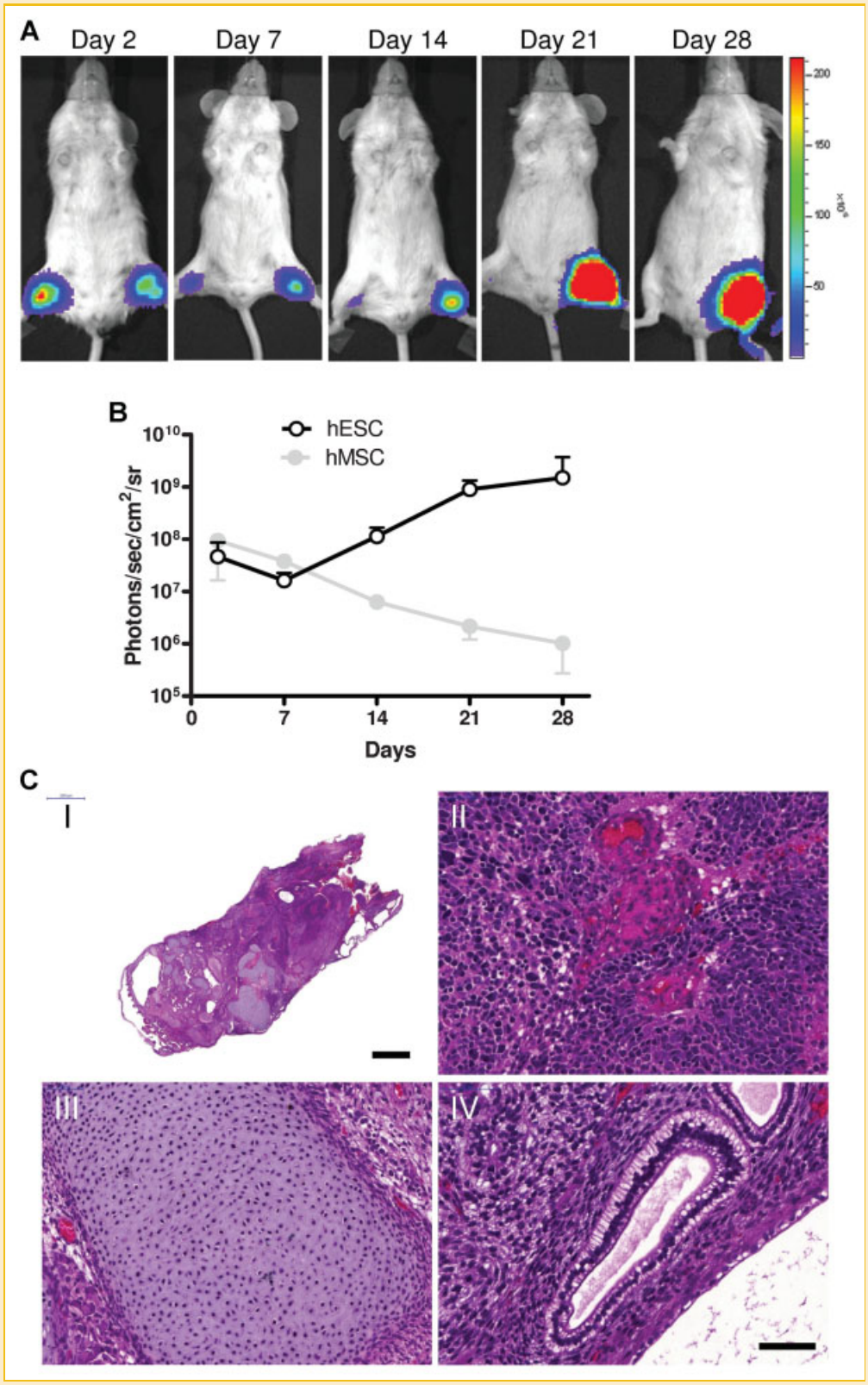

Fig. 2. Imaging and histologic analysis of hES cells fate after transplantation. A: Representative animal injected with 1×10^6 MSCs (right hind limb) showed significant bioluminescence activity on day 2 after transplantation, which decreased progressively during the following 4 weeks. In contrast, undifferentiated hES cells (left hind limb) showed the lowest bioluminescence signals on day 7, which had increased dramatically between weeks 2 and 4. B: Detailed quantitative analysis of signals from all animals transplanted with hES cells versus MSCs. Signal activity is expressed as photons/s/cm^2/sr. C: Histologic analysis of double labeled hES cells. H&E staining of teratoma formation (I) after hES cell implantation identified various cell types containing tissues of all three embryonic germ layers, such as (II) neural epithelium (ectoderm), (III) osteoid formation (mesoderm), and (IV) gut epithelium (endoderm). Scale bar = 2,000 μm (I) and 20 μm (II–IV).

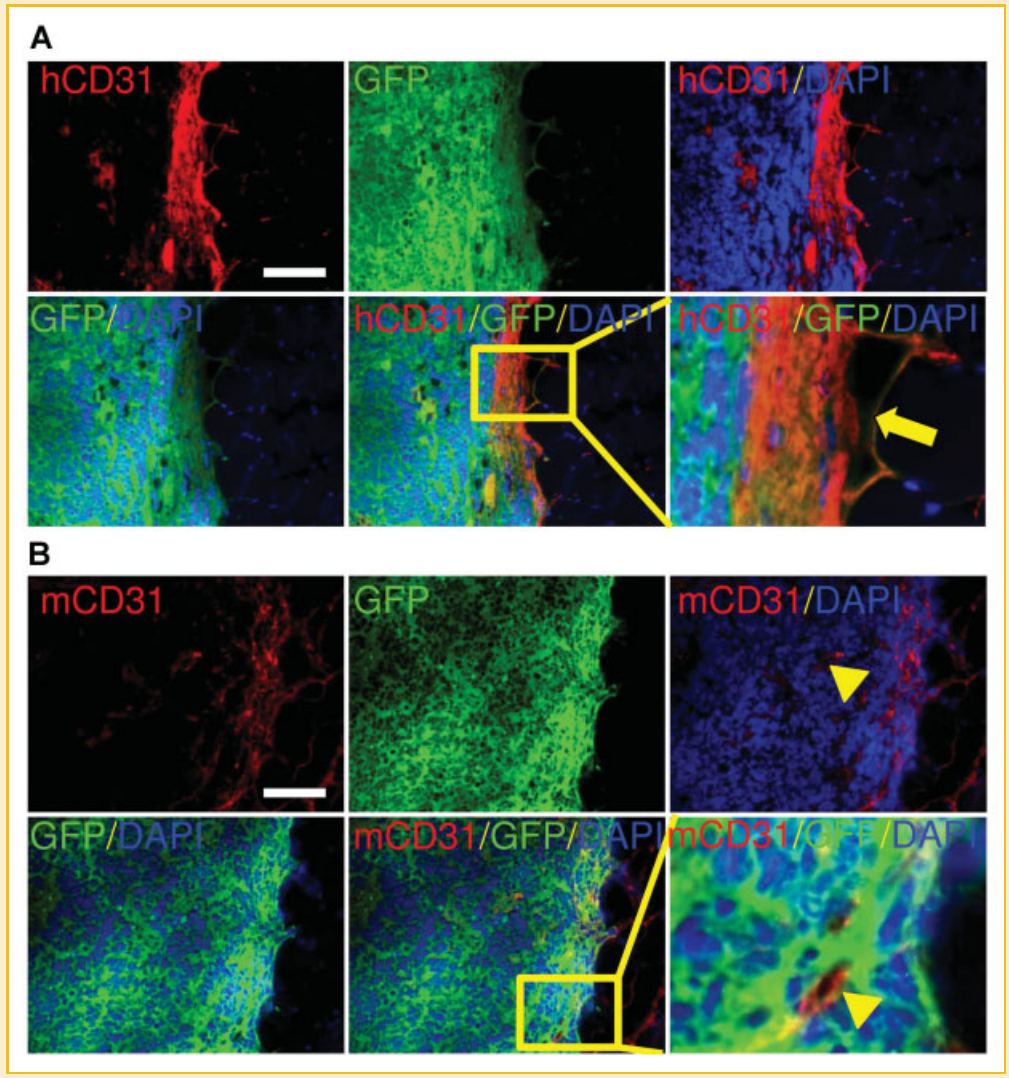

Fig. 3. Demonstration of angiogenesis in teratoma. A: Immunofluorescence staining for GFP and human CD31 on week 4 after transplantation of hES cells. GFP expression indicates that cells were derived from hES cells and human CD31 expression suggests endothelial differentiation of hES cells in vivo. The transplanted GFP^+ hES cells revealed endothelial differentiation and integrating into host vasculatures. Scale bar = 100 μm. B: Immnostaining of teratoma formation of transplanted double fusion hES cells for GFP and mouse CD31. Mouse CD31 expression indicates that cells which formed the microvasculature of teratoma did come from the mouse itself. Nuclei were stained with DAPI (blue). Mouse CD31 positive cells were detected in teratoma, implying that host vasculatures expanded into teratoma. Scale bar = 100 μm.

are showing some promise [Kerbel, 2008]. By immunostaining, we observed that vasculature formation from hES cells was confirmed by GFP and human CD31 double positive on teratoma, indicating endothelial differentiation of the transplanted GFP positive hES cells in vivo. We also found that vascular networks expanding from host were confirmed by mouse CD31 staining inside the teratoma, indicating that host vasculatures spreading into teratoma actually promote teratoma growth by supplying nutrients. With regard to the clinical application of hES-derived cells, teratoma formation remains a significant concern. Based on successful vascular targeting therapies in oncology, we believe that both agents targeting endothelial cells differentiated from hES cells and preventing host vasculatures from expanding into teratoma may be a practical choice to prevent and treat teratoma formed by undifferentiated hES cells.

Formation of three somatic germ layers within teratoma is considered the best indicator of the pluripotency of hES cell lines [Lensch et al., 2007; Blum et al., 2009]. A further understanding of this process should aid in the development of safer hES cell therapies and may help elucidate the principles of teratoma formation. Thus, our FACS data revealed for the first time that CD56 is expressed robustly in teratoma-derived cells. CD56, a 200–220 kDa cell surface glycoprotein, has been identified as an isoform of the neural adhesion molecules, and was found frequently expressed on the surface of neurons, glia, skeletal muscle, and natural killer (NK) cells, as well as in several lympho-hematopoietic neoplasms [Raspadori et al., 2001; Kurokawa et al., 2003; Kontogianni et al., 2005; Ohishi et al., 2007; Pruszak et al., 2007]. CD56 also is intensely expressed in the mesenchyme [Jin et al., 1991] and a marker of early neuro-ectodermal

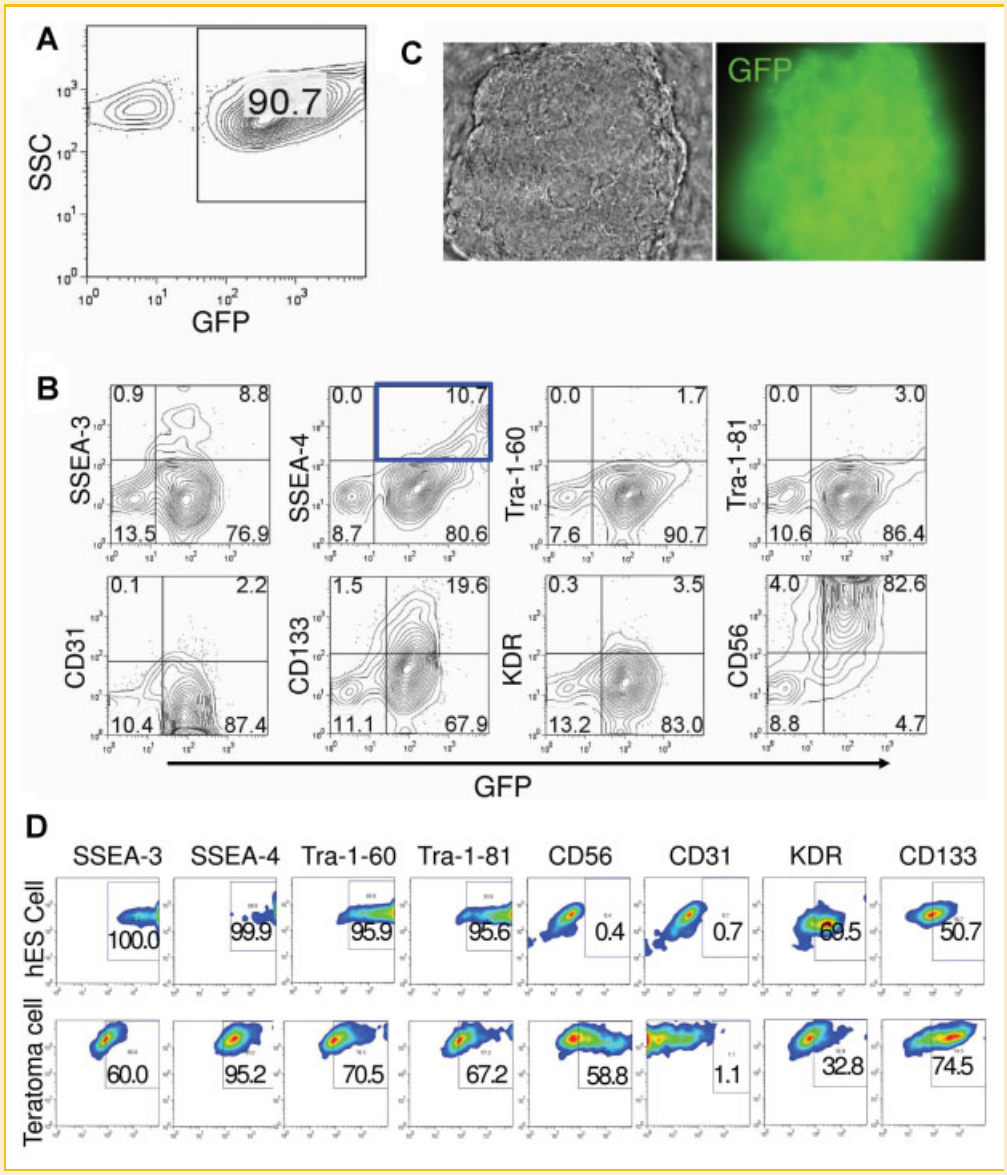

Fig. 4. In vitro characterization of teratoma-derived cells. A: Flow cytometric analysis showed that most teratoma-derived cells were GFP positive, indicating that such cells derived from hES cells. B: Flow cytometric analysis revealed that teratoma-derived cells expressed a panel of differentiated and undifferentiated markers. Especially, CD56 and undifferentiated marker SSEA-4 were expressed at high levels. C: In vitro subculture of GFP$^+$/SSEA-4$^+$ teratoma-derived cells is depicted whose morphology was like that of undifferentiated hES cells. D: Characterization of subcultured GFP$^+$/SSEA-4$^+$ cells isolated from teratoma with hES cells being used as a positive control. These results indicate that subcultured GFP$^+$/SSEA-4$^+$ cells had similar expression pattern when compared to undifferentiated hES cells, but did express very high levels of CD56 and a somewhat lower expression of undifferentiated markers, such as SSEA-3, SSEA-4, TRA-1-60, and TRA-1-81. Single representative sample of triplicate analysis are shown.

differentiation [Reubinoff et al., 2001], which has been used to identify neural differentiation of hESCs by flow-cytometric analysis and sorting [Pruszak et al., 2007; Sundberg et al., 2009]. Consequently, we suggest that the expression of CD56 following hES cell transplantation in vivo may indicate the teratoma formation with a large degree of embryonic neural derivatives.

As far as histopathology is concerned, teratomas are characterized as either mature and benign or as immature and malignant [Lensch et al., 2007]. Even though there are well-defined somatic structures in hES-derived teratoma, undifferentiated tissue may be noted and should be considered and evaluated to archive future successful hES cell therapy. Thus, our FACS data showed that teratoma-derived cells expressed undifferentiated markers SSEA-3, SSEA-4, as well as Tra-1-60, Tra-1-81. Moreover, in vivo transplantation indicated that such cells exhibited multipotency, but their proliferation activity was not very high compared to hES cells by BLI. However, H&E staining showed nuclear enlargement and increased nuclear-to-cytoplasmic ratio in hES cells derived teratoma. In contrast, the presence of more differentiated cells with lower nuclear-to-cytoplasmic ratio in teratoma-derived neoplasia indicates that teratoma is a benign, multidifferentiated tissue which contains immature, but not

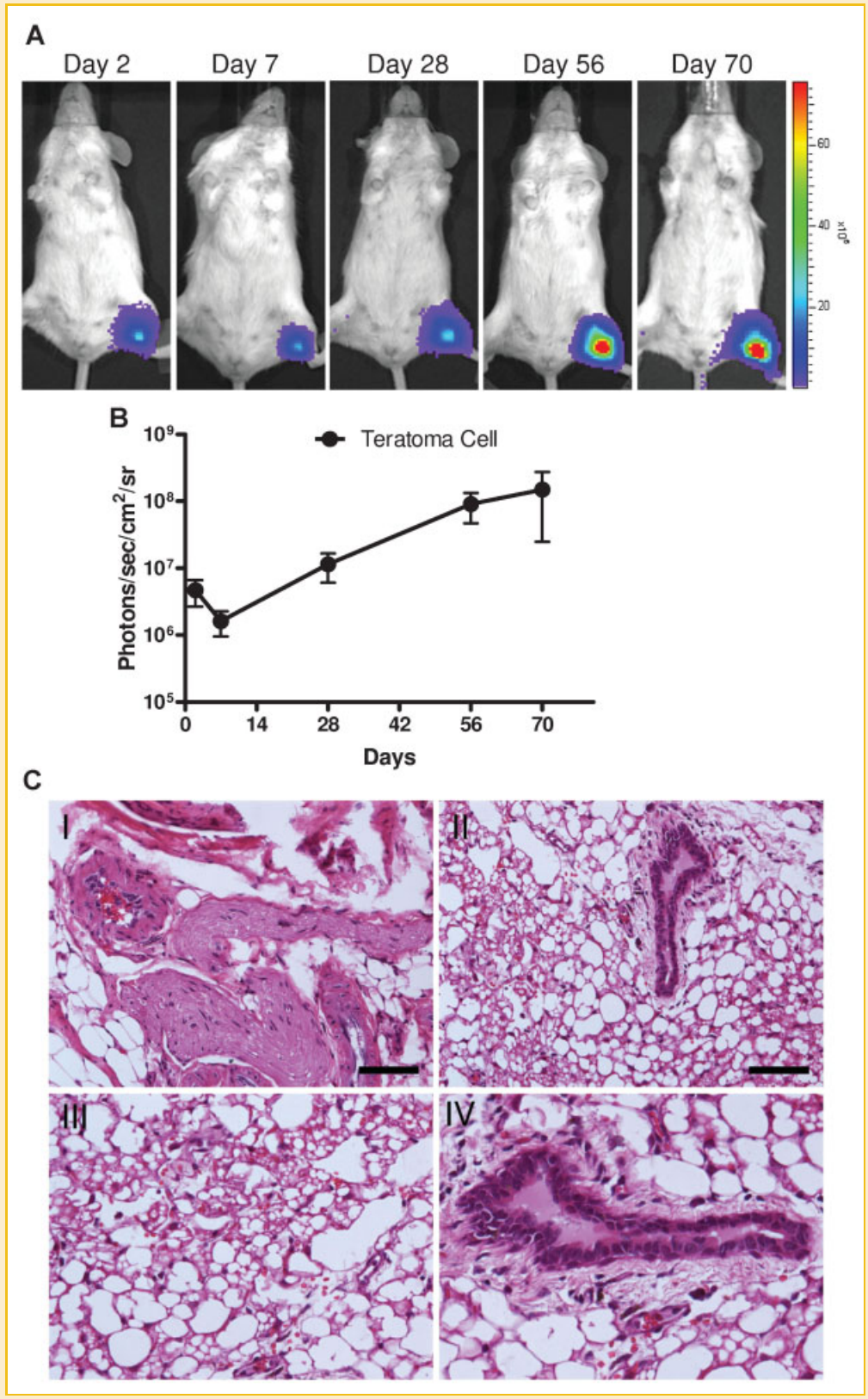

Fig. 5. Reporter gene imaging and histologic analysis of the fate of $GFP^+/SSEA\text{-}4^+$ cells after transplantation. A: Representative animal was injected into the left hind limb with 1×10^6 $GFP^+/SSEA\text{-}4^+$ teratoma-derived cells (left hind limb) showed significant bioluminescence activity on day 2, which decreased during the first 7 days, then increased progressively over the following 10 weeks. B: Detailed quantitative analysis of signals from all animals transplanted with $GFP^+/SSEA\text{-}4^+$ cells. Signal activity is expressed as photons/s/cm^2/sr. C: H&E staining of teratoma formation is shown. Upon injection into SCID mice, $GFP^+/SSEA\text{-}4^+$ teratoma-derived cells again formed teratoma-like neoplasms in vivo, which contained tissues from all three embryonic germ layers, including (I) neural epithelium (ectoderm), (II) mesoderm and endoderm, (III) adipose tissue (mesoderm), and (IV) gut epithelium (endoderm). Scale bar = 20 μm (I, III, and IV) and 40 μm (II).

malignant cells. Of note, the teratoma-derived cells were capable of forming teratoma-like masses and proliferated at low level in vivo, an indication of incomplete pluripotency as compared to hES cells.

In summary, our study demonstrates that BLI can be used to monitor aberrant behavior of hES cells noninvasively in living animals. FACS analysis revealed that teratoma derived from hES cells expressed high levels of CD56, which is a good indicator for teratoma formation from hES cells in vivo. Moreover, teratoma tissues were composed of undifferentiated cell populations, which expressed SSEA-3, SSEA-4, Tra-1-60, and Tra-1-81. However, this cell population was more differentiated and had less proliferating capacity than hES cells that would have more difficulty to form teratoma-like masses in vivo.

ACKNOWLEDGMENT

This work was funded by National Key Scientific Program of China (2011CB964903) to ZL and DK; National Natural Science Foundation of China (31071308) to ZL; National Development Plan of High Technology of China (2007AA021010); National Key Scientific Program of China (2007CB914804), Key Program of National Natural Science Foundation of China (30830096) and China-Sweden Joint Key Program from Tianjin Municipal Science and Technology Commission (09ZCZDSF04000) to RX; and grants from the National Institutes of Health (HL091453, AI085575) to JCW.

REFERENCES

Blum B, Bar-Nur O, Golan-Lev T, Benvenisty N. 2009. The anti-apoptotic gene survivin contributes to teratoma formation by human embryonic stem cells. Nat Biotechnol 27:281–287.

Hentze H, Soong PL, Wang ST, Phillips BW, Putti TC, Dunn NR. 2009. Teratoma formation by human embryonic stem cells: Evaluation of essential parameters for future safety studies. Stem Cell Res 2:198–210.

Jin L, Hemperly JJ, Lloyd RV. 1991. Expression of neural cell adhesion molecule in normal and neoplastic human neuroendocrine tissues. Am J Pathol 138:961–969.

Kerbel RS. 2008. Tumor angiogenesis. N Engl J Med 358:2039–2049.

Kontogianni K, Nicholson AG, Butcher D, Sheppard MN. 2005. CD56: A useful tool for the diagnosis of small cell lung carcinomas on biopsies with extensive crush artefact. J Clin Pathol 58:978–980.

Kurokawa M, Nabeshima K, Akiyama Y, Maeda S, Nishida T, Nakayama F, Amano M, Ogata K, Setoyama M. 2003. CD56: A useful marker for diagnosing Merkel cell carcinoma. J Dermatol Sci 31:219–224.

Lensch MW, Schlaeger TM, Zon LI, Daley GQ. 2007. Teratoma formation assays with human embryonic stem cells: A rationale for one type of human-animal chimera. Cell Stem Cell 1:253–258.

Li Z, Wu JC, Sheikh AY, Kraft D, Cao F, Xie X, Patel M, Gambhir SS, Robbins RC, Cooke JP, Wu JC. 2007. Differentiation, survival, and function of embryonic stem cell derived endothelial cells for ischemic heart disease. Circulation 116:I46–54.

Li Z, Suzuki Y, Huang M, Cao F, Xie X, Connolly AJ, Yang PC, Wu JC. 2008. Comparison of reporter gene and iron particle labeling for tracking fate of human embryonic stem cells and differentiated endothelial cells in living subjects. Stem Cells 26:864–873.

Li Z, Han Z, Wu JC. 2009a. Transplantation of human embryonic stem cell-derived endothelial cells for vascular diseases. J Cell Biochem 106:194–199.

Li Z, Lee A, Huang M, Chun H, Chung J, Chu P, Hoyt G, Yang P, Rosenberg J, Robbins RC, Wu JC. 2009b. Imaging survival and function of transplanted cardiac resident stem cells. J Am Coll Cardiol 53:1229–1240.

Li Z, Wilson KD, Smith B, Kraft DL, Jia F, Huang M, Xie X, Robbins RC, Gambhir SS, Weissman IL, Wu JC. 2009c. Functional and transcriptional characterization of human embryonic stem cell-derived endothelial cells for treatment of myocardial infarction. PLoS One 4:e8443.

Ohishi Y, Kaku T, Oya M, Kobayashi H, Wake N, Tsuneyoshi M. 2007. CD56 expression in ovarian granulosa cell tumors, and its diagnostic utility and pitfalls. Gynecol Oncol 107:30–38.

Phillips BW, Hentze H, Rust WL, Chen QP, Chipperfield H, Tan EK, Abraham S, Sadasivam A, Soong PL, Wang ST, Lim R, Sun W, Colman A, Dunn NR. 2007. Directed differentiation of human embryonic stem cells into the pancreatic endocrine lineage. Stem Cells Dev 16:561–578.

Pruszak J, Sonntag KC, Aung MH, Sanchez-Pernaute R, Isacson O. 2007. Markers and methods for cell sorting of human embryonic stem cell-derived neural cell populations. Stem Cells 25:2257–2268.

Raspadori D, Damiani D, Lenoci M, Rondelli D, Testoni N, Nardi G, Sestigiani C, Mariotti C, Birtolo S, Tozzi M, Lauria F. 2001. CD56 antigenic expression in acute myeloid leukemia identifies patients with poor clinical prognosis. Leukemia 15:1161–1164.

Reubinoff BE, Itsykson P, Turetsky T, Pera MF, Reinhartz E, Itzik A, Ben-Hur T. 2001. Neural progenitors from human embryonic stem cells. Nat Biotechnol 19:1134–1140.

Sundberg M, Jansson L, Ketolainen J, Pihlajamäki H, Suuronen R, Skottman H, Inzunza J, Hovatta O, Narkilahti S. 2009. CD marker expression profiles of human embryonic stem cells and their neural derivatives, determined using flow-cytometric analysis, reveal a novel CD marker for exclusion of pluripotent stem cells. Stem Cell Res 2:113–124.

Thomson JA, Itskovitz-Eldor J, Shapiro SS, Waknitz MA, Swiergiel JJ, Marshall VS, Jones JM. 1998. Embryonic stem cell lines derived from human blastocysts. Science 282:1145–1147.

Xu CH, He JQ, Kamp TJ, Police S, Hao XM, O'Sullivan C, Carpenter MK, Lebkowski J, Gold JD. 2006. Human embryonic stem cell-derived cardiomyocytes can be maintained in defined medium without serum. Stem Cells Dev 15:931–941.

Xu XQ, Zweigerdt R, Soo SY, Ngoh ZX, Tham SC, Wang ST, Graichen R, Davidson B, Colman A, Sun W. 2008. Highly enriched cardiomyocytes from human embryonic stem cells. Cytotherapy 10:376–389.

Zhao QJ, Ren HY, Li XY, Chen Z, Zhang XY, Gong W, Liu YJ, Pang TX, Han ZC. 2009. Differentiation of human umbilical cord mesenchymal stromal cells into low immunogenic hepatocyte-like cells. Cytotherapy 11:414–426.